frontiers | Frontiers in Earth Science

TYPE Original Research
PUBLISHED 21 July 2025
DOI 10.3389/feart.2025.1613160

OPEN ACCESS

EDITED BY
Rui Liu,
University of Canberra, Australia

REVIEWED BY
Yali Zhu,
Chinese Academy of Sciences (CAS), China
Qianrong Ma,
Yangzhou University, China

*CORRESPONDENCE
Cailian Jiang,
jcl-qxj@163.com

RECEIVED 16 April 2025
ACCEPTED 24 June 2025
PUBLISHED 21 July 2025

CITATION
Li J, Li B, Jiang C, Jiang Y, Zhang J, Yang L and Li N (2025) A case study of extreme rainstorm in northern Xinjiang under the influence of large-scale circulation and topography. *Front. Earth Sci.* 13:1613160. doi: 10.3389/feart.2025.1613160

A case study of extreme rainstorm in northern Xinjiang under the influence of large-scale circulation and topography

Jiangang Li[1,2,3,4], Boyuan Li[5], Cailian Jiang[6]*, Yufei Jiang[1,2,3,4], Jinru Zhang[1,2,3,4], Lianmei Yang[1,2,3,4] and Na Li[7]

[1]Institute of Desert Meteorology, China Meteorological Administration, Urumqi, Xinjiang, China, [2]Xinjiang Innovation Institute of Cloud Water Resource Development and Utilization, Urumqi, China, [3]Xinjiang Cloud Precipitation Physics and Cloud Water Resources Development Laboratory, Urumqi, Xinjiang, China, [4]Field Scientific Observation Base of Cloud Precipitation Physics in West Tianshan Mountains, Urumqi, Xinjiang, China, [5]Altai Meteorological Bureau of Xinjiang Uygur Autonomous Region, Altai, Xinjiang, China, [6]Wujiaqu Meteorological Bureau of the Sixth Division, Xinjiang Production and Construction Corps, Wujiaqu, Xinjiang, China, [7]Xinjiang Meteorological Observatory, Urumqi, Xinjiang, China

Introduction: Heavy rainfall events in Northern Xinjiang are primarily influenced by westerly systems, exhibiting strong extremity, which exacerbate secondary disasters. Meteorologists have conducted in-depth research on the trigger mechanisms, atmospheric backgrounds, meso- and microscale features, forecasting and warning techniques and environmental impacts of heavy rainfall events. Based on the automated weather station data, FY-4A satellite products, ECWMF model sounding data, NCEP-FNL and ERA5 reanalysis datasets, this study analyzes the environmental field characteristics of an extreme regional heavy rainfall event in Northern Xinjiang from August 7–9, 2023.

Methods: The heavy rainfall and short-term heavy rainfall were defined according to Xinjiang local precipitation standards, reanalysis datasets were primarily used to circulation patterns, water vapor transport, thermodynamic conditions and etc. Satellite products were utilized for cloud-top brightness temperature and water vapor convergence monitoring and analysis.

Results: The results indicated that the heavy rainfall occurred under the circulation background of the eastern-type South Asian High. Influenced by the upstream European blocking high and downstream East Siberian ridge, the West Siberian trough merged with the Central Asian trough. Shortwave troughs propagating eastward ahead of this merged system continuously entered Northern Xinjiang, interacting with a strong and persistent low-level southwest jet stream convergence zone to trigger widespread heavy rainfall. Atmospheric stratification characterized by warm lower layers and cold upper layers, mesoscale convergence induced by low-level wind shear lines, and the presence of high-energy zones facilitated the release of substantial convective unstable energy. This triggered the rapid development and maintenance of Meso-β-scale convective cloud clusters, resulting in localized short-duration precipitation. Water vapor was primarily transported via the dominant western channel, supplemented by the eastern channel. Stable synoptic systems enabled significant water vapor to reach the heavy rainfall area in advance. The western

boundary contributed to full-layer water vapor input, while the southern boundary provided mid-to-upper-level input, leading to increased water vapor flux, enhanced convergence, and prolonged saturation. Influenced by local topography, low-level wind convergence, and a dual-center vertical velocity and divergence configuration with a forward-tilted structure rapidly intensified precipitation.

Discussion: This study reveals that the cause of the heavy rainfall event in northern Xinjiang is the synergy of multi-scale systems under the background of abnormal circulation in Central Asia: the eastward-moving South Asian High (SAH) drives the southwest jet stream to extend southward, and in combination with the European blocking high (584-588 dagpm), it prompts the split of the Central Asian trough and the eastward movement of the short-wave trough. The rainstorm area shows a vertical structure of "cold above and warm below", strong vertical wind shear and high CAPE value (>2500 J/kg), triggering deep convective cloud clusters with TBB ≤ -40°C. An innovative discovery of the double-channel water vapor convergence mechanism upstream and downstream is made, and combined with the uplift of the Altai Mountains, the water vapor flux and convergence intensity in front of the mountains are significantly higher than those of historical events. Satellite data verify its monitoring potential and resolution limitations in radar blind areas. This event confirms that the rapid eastward movement of the short-wave trough and the terrain-triggered mesoscale convection are the key factors causing disasters, emphasizing the need to establish a refined early warning system for mountain floods.

KEYWORDS

northern Xinjiang, regional heavy rainfall, atmospheric circulation, water vapor transport, geostationary satellite

1 Introduction

Northern Xinjiang, bordered by the Tianshan Mountains to the south and the Altai Mountains to the north, features a temperate continental arid and semi-arid climate. Heavy rainfall events in this region are primarily influenced by westerly systems, differing significantly from those in eastern China. These events exhibit strong extremity, with the precipitation from single heavy rainfall process sometimes approaching or exceeding annual averages (Li et al., 2022; Zhang and Deng, 1987). Mountainous terrain and sparse vegetation exacerbate secondary disasters such as flash floods and landslides. Accurate heavy rainfall forecasting is critical for water resource management and disaster mitigation.

Over the years, domestic and international meteorologists have conducted in-depth research on the trigger mechanisms (Keim, 2010; Song et al., 2015; Zhao et al., 2017; Ziv, 2001), atmospheric backgrounds (Bradley and Smith, 1994; Chen et al., 2010; Morin et al., 2007; Yu and Meng, 2016), meso- and micro-scale features (Hirockawa and Kato, 2012; Houze et al., 1990; Shin and Lee, 2015; Sun et al., 2015), forecasting and warning techniques (Chessa et al., 2003; Lapo et al., 2017; Trivedi et al., 2024; Wang et al., 2023; Yadav et al., 2021), and environmental impacts (Bull et al., 2000; Gregersen et al., 2014; Hyun et al., 2007; Lima and Singh, 2002) of heavy rainfall events, yielding significant achievements.

For Xinjiang, researchers have extensively studied the causes of heavy rainfalls, water vapor transport, and related environmental conditions (Japay et al., 2007; Jiang et al., 2013; Jiang and Qin, 2024; Kong et al., 2011; Yang, 2003; Zeng et al., 2019; Zhang and Wang, 2004). These studies established a synoptic conceptual model for large-scale heavy rainfalls in Xinjiang, characterized by dual-pattern South Asian High at 100 hPa and a subtropical longwave trough at 500 hPa as the circulation background; typical configuration of upper-level southwest jets, mid-level southerly jets, and low-level easterly jets; Relay water vapor transport from the Atlantic, Mediterranean, Black Sea, Central Asia, and Southwest Asia to the region (with low-level water vapor contributing most to heavy rainfalls); Meso- and micro-scale convergence in the mid-to-low troposphere triggering convection and heavy rainfall. While previous studies focused more on Southern Xinjiang, research on northern Xinjiang heavy rainfall remains limited.

In the condition of a small number and extremely uneven distribution of automatic weather stations, and a large blind spot in weather radar coverage, so the use of high-resolution satellite data is particularly important for monitoring and analyzing hazardous weather. Satellite data is not limited by geography and time, especially geostationary meteorological satellites. This paper utilizes multi-source data, including conventional observation data, high-resolution meteorological satellite products, and reanalysis datasets to conduct a detailed analysis of the causes of a typical heavy rainfall event in Northern Xinjiang during the summer of 2023. The aim is to establish early warning indicators for heavy rainfall in the region, providing theoretical support for local disaster prevention and migration, ecological conservation, and sustainable development.

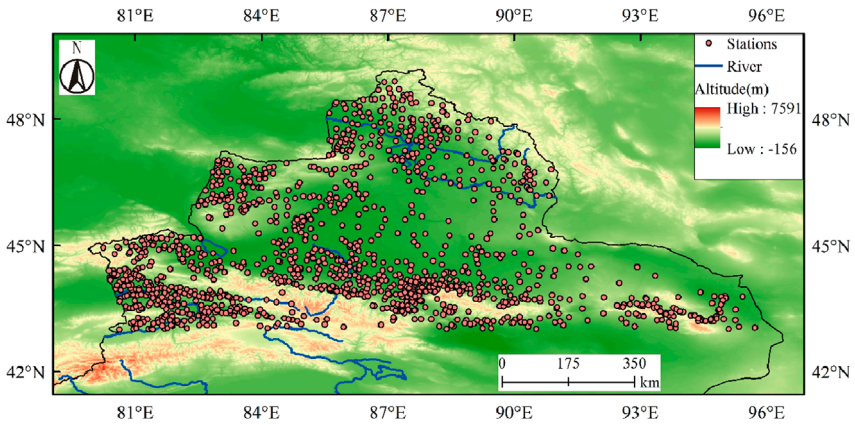

FIGURE 1
The topography and meteorological stations in Northern Xinjiang.

2 Data

Northern Xinjiang primarily includes: the Ili Kazakh Autonomous Prefecture (abbreviated as Ili Prefecture, encompassing Ili, Tacheng, and Altai regions), Bortala Mongol Autonomous Prefecture (abbreviated as Bortala Prefecture, hereinafter), Changji Hui Autonomous Prefecture (abbreviated as Changji Prefecture, hereinafter), Karamay City, Shihezi City, and Urumqi City. This area contains more than 1,300 meteorological sites (Figure 1).

The observational data used in this study were sourced from the China Meteorological Administration's "Sky-Engine" Big Data Platform, providing hourly precipitation records from meteorological stations in Northern Xinjiang. Gridded data include three types: NCEP/FNL reanalysis (Deng et al., 2009) (spatial resolution: 1° × 1°, temporal resolution: 6-hourly); ERA5 reanalysis (Dragani et al., 2015) (spatial resolution: 0.25° × 0.25°, temporal resolution: hourly); ECMWF high-resolution model soundings (Stankov, 1998) (spatial resolution: 0.25° × 0.25°, temporal resolution: 3-hourly).

Satellite data (spatial resolution: 4 km; temporal resolution: 6 or 15 min) were chosen from the FY-4A (Fengyun-4A) geostationary meteorological satellite, one of China's new-generation geostationary satellite series launched in 2016, which sub-satellite point is currently positioned at 123.5°E (originally at 104.7°E). The TBB (Brightness Temperature of Black Body, unit: K, hereinafter) and LPW (Layered Precipitable Water, unit: g/kg, hereinafter) products were used in this paper.

All times referenced in this paper are in GMT (Greenwich Mean Time), which is approximately 5 h behind the local time.

3 Methodology

Daily precipitation in this study were calculated using the internationally recognized standard from 12:00 GMT on the previous day to 12:00 GMT on the following day. Due to the unique climatic conditions of Xinjiang, the criteria for defining heavy rainfall and short-term heavy rainfall were based on the Xinjiang local precipitation standards (Dolaite, 2005; Zhuang et al., 2024). This approach highlights the extreme nature of the precipitation event.

The NCEP/FNL reanalysis data were primarily used to analyze large-scale circulation patterns, water vapor transport, and budget calculations. ERA5 data were employed to investigate hourly water vapor and thermodynamic conditions at the rainfall center. ECWMF (European Centre for Medium-Range Weather Forecasts) model sounding data, which have been widely applied for many years to produce forecast products, analyze and summarize weather processes, and write decision service materials, were used for characterize atmospheric instability stratification and convective parameters in the precipitation center.

To examine the evolution of convective cloud systems during this heavy rainfall event, FY-4A/TBB products were utilized for cloud-top brightness temperature and water vapor convergence monitoring and analysis. This product includes eight spectral channels, with the long-wave infrared Channel 12 (spectral bandwidth: 10.3–11.3 μm) and long-wave infrared Channel 11 (spectral bandwidth: 8.0–9.0 μm) selected for the TBB value and water vapor transportation calculation respectively.

4 Research results

4.1 Overview of the rainfall process

From 7 to 9 August 2023, heavy precipitation occurred in multiple areas of Northern Xinjiang. According to the cumulative process precipitation, 69 stations recorded rainfall reaching the *heavy rainfall* threshold, and 5 stations reached the *torrential rainfall* threshold, primarily distributed in the Ili, Bortala Prefecture, and Altay region (Figure 1). The primary and secondary precipitation centers were both located in the Altay region (Qibeiling Reservoir and Kala Wengger Village, abbreviation of Qibeiling and Kala stations respectively, hereinafter), with

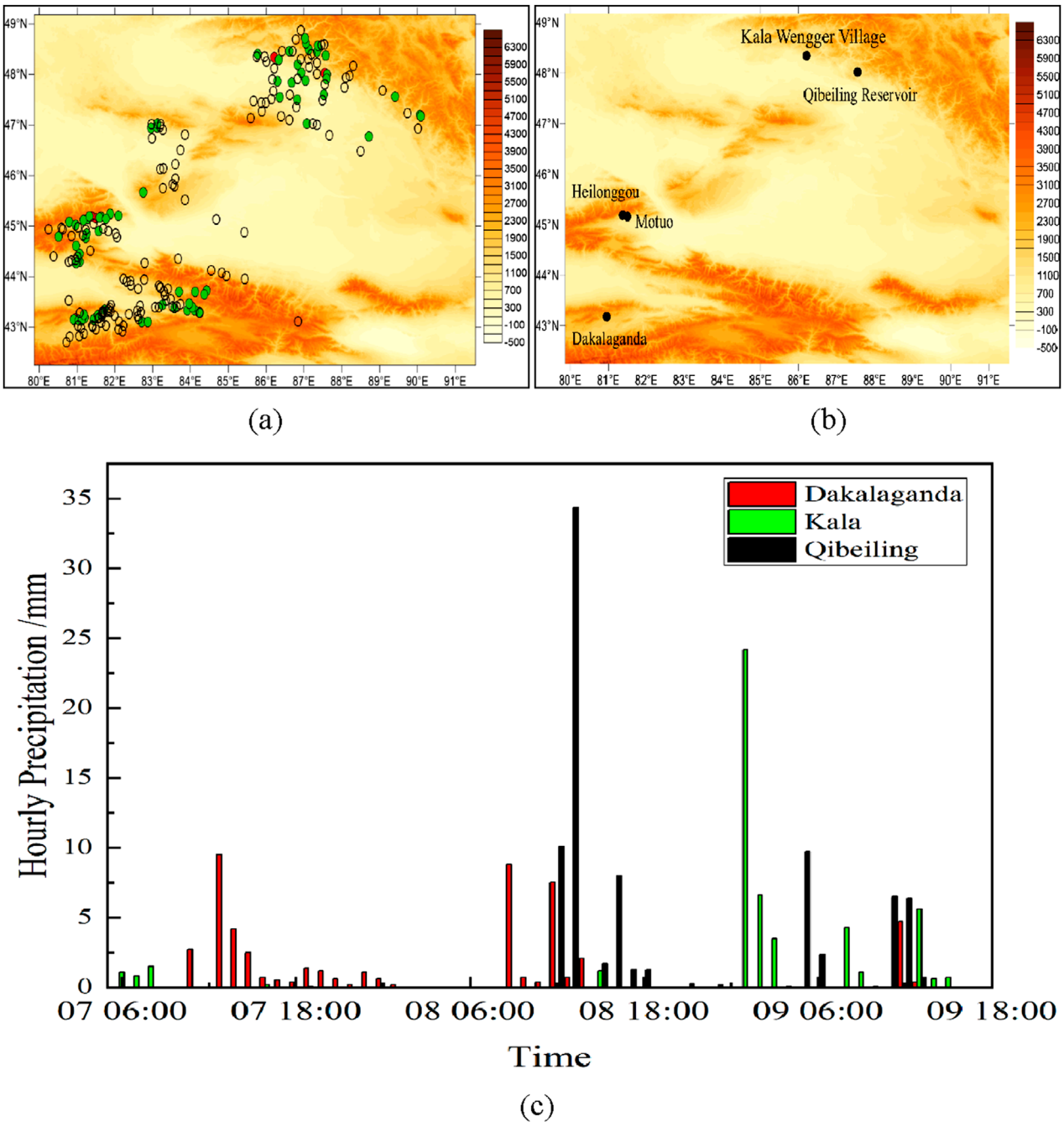

FIGURE 2
(a) Cumulative process precipitation distribution (unit: mm) from 00:00 August 7 to 00:00 August 10, 2023 (● represents stations with process cumulative precipitation >48.0 mm, ● for 24.1–48.0 mm, and ○ for <24.1 mm); **(b)** Distribution of stations with cumulative precipitation >48.0 mm (● represents stations); **(c)** Hourly precipitation distribution (unit: mm/h) for the top three stations.

total accumulated precipitation amounts correspond to 83.0 mm and 51.8 mm (Figure 2b).

In terms of daily precipitation distribution, 27 stations within the study area recorded daily rainfall reached the *heavy rainfall* criteria, mainly concentrated in the Altay Region (16 stations) and Ili Prefecture (7 stations). The Qibeiling Station recorded 57.3 mm, classified as torrential rainfall. Additionally, short-duration intense rainfall occurred at multiple stations, predominantly in the Altay region (31 stations) and Ili Prefecture (10 stations). Stronger short-duration rainfall (≥20.0 mm) was primarily observed in the Altay Region (10 stations), with the maximum intensity recorded at Qibeiling Station (44.5 mm rainfall in 2 h) between 11:00 a.m. and 13:00 p.m. on 8 August (Figure 2c). Consequently, the Altay Region, where heavy rainfall and short-term heavy rainfall were most concentrated, was selected as the key research area.

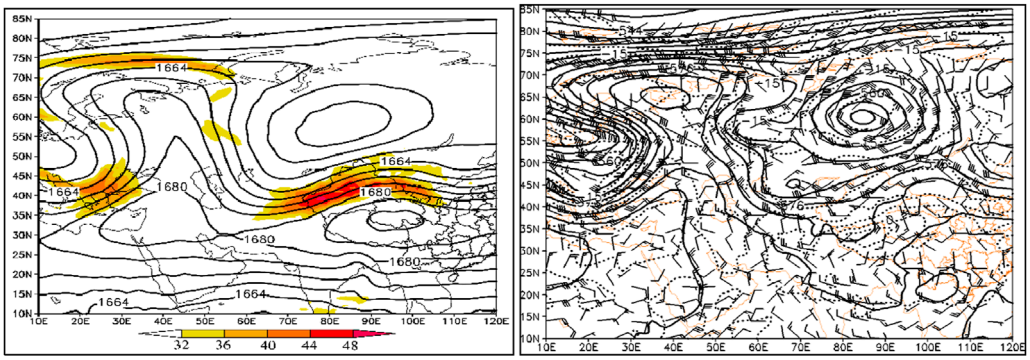

FIGURE 3
Geopotential height fields at 00:00 on August 8, 2023: **(a)** 200 hPa (solid lines: geopotential height, unit: dagpm; shaded areas: jet streams). **(b)** 500 hPa (solid lines: geopotential height, unit: dagpm; dashed lines: temperature field, unit: °C; superimposed wind field, unit: $m{\cdot}s^{-1}$).

4.2 Atmospheric circulation and mesoscale characteristics

4.2.1 Atmospheric circulation

Based on the analysis of circulation evolution during this event, the South Asian High (SAH) at the 100 hPa level transitioned from a bimodal pattern before the rainstorm to an eastern mode during the event, with its intensity gradually strengthening, and its center located over the Tibetan Plateau. At 00:00 GMT on August 8, Northern Xinjiang was located in the divergence zone on the left side of the 200 hPa upper-level southwestern jet stream axis (wind speed >30 $m{\cdot}s^{-1}$). The jet stream intensified progressively, reaching its peak strength (with jet core of 56 $m{\cdot}s^{-1}$) at 06:00 on August 9, and then slightly weakened. The rainstorm area remained within the divergence zone on the left side of the upper-level southwestern jet stream axis (figure omitted). The establishment and persistence of the SAH's eastern mode facilitated the formation, maintenance, and southward extension of the southwestern jet stream ahead of the long-wave trough.

At 500 hPa, the upstream Iranian subtropical high and the South European ridge combined to form a robust European blocking high. Downstream, the Western Pacific subtropical high and the East Siberian ridge were in phase, further hindering the eastward movement of influencing systems. This configuration promoted the southward development and westward retreat of the Siberian low vortex, amplifying the meridionality of circulation. The short-wave troughs continuously splitting from the base of the low vortex merged with the Central Asian trough, triggering the rapid eastward movement of systems that ultimately caused this rainstorm event.

At lower 700 hPa atmospheric Level: The southerly jet stream over northern Xinjiang gradually shifted to a southwesterly jet stream and remained within the convergence zone at the jet's leading edge. A persistent shear line was observed near the Qibeiling Station, transitioning from west-southwesterly wind shear before the rainstorm to northwesterly-southwesterly wind shear during the event. Westerly wind convergence was prominent both before and during the rainstorm, weakening in intensity after the event. Southwesterly winds persisted over the rainstorm-affected area, forming convergent uplift of moderate intensity ahead of the northwest-southeast oriented Altai Mountains, which enhanced precipitation intensity at 850 hPa (Figure 3).

On the surface, a distinct mesoscale shear line existed upstream of the Qibeiling Station. By 11:00 GMT, easterly winds developed at Qibeiling and stations to its east, creating west-east directional convergence and easterly wind speed convergence. As the easterly winds strengthened, the shear-induced convergence peaked, triggering short-duration heavy rainfall. By 13:00 GMT, the convergence weakened significantly, leading to a notable reduction in precipitation (Figure 4).

4.2.2 Characteristics of mesoscale convective cloud clusters

The rapid eastward movement of a shortwave trough ahead of the Central Asian trough initiated local convective activity. The FY-4A/TBB distribution revealed continuous development of convective cloud clusters ahead of the trough, generally exhibiting a cyclonic distribution from northwest to southwest, which rapidly moved eastward, causing heavy rainfall across northern Xinjiang. Around 19:30 on the 8th, a meso-γ scale convective cloud cluster (MγCS) with a horizontal scale less than 20 km formed due to frontal genesis southeast of Qibeiling Station, with a TBB of −32°C. Enhanced by the convergence of low-level wind fields, the cold cloud shield expanded in area and intensified, evolving into an elongated meso-β scale convective system ($M_{\beta}ECS$) by 20:00, which remained quasi-stationary. By 20:30, the cloud cluster began cyclonic rotation, strengthened into a nearly circular meso-β scale convective system ($M_{\beta}CCS$), and moved northeastward to the area above northeastern Qibeiling Station. The TBB at its center reached −40°C, with Qibeiling Station located in the southwestern region of the MCS cloud cluster where the brightness temperature gradient was steep. This timing coincided with the occurrence of heavy rainfall on the surface (Figure 5).

4.3 Atmospheric stratification

The heavy rainfall area was mainly concentrated in the Altay region, which has only one sounding station (Altay Station). Therefore, the atmospheric stratification conditions at Qibeiling

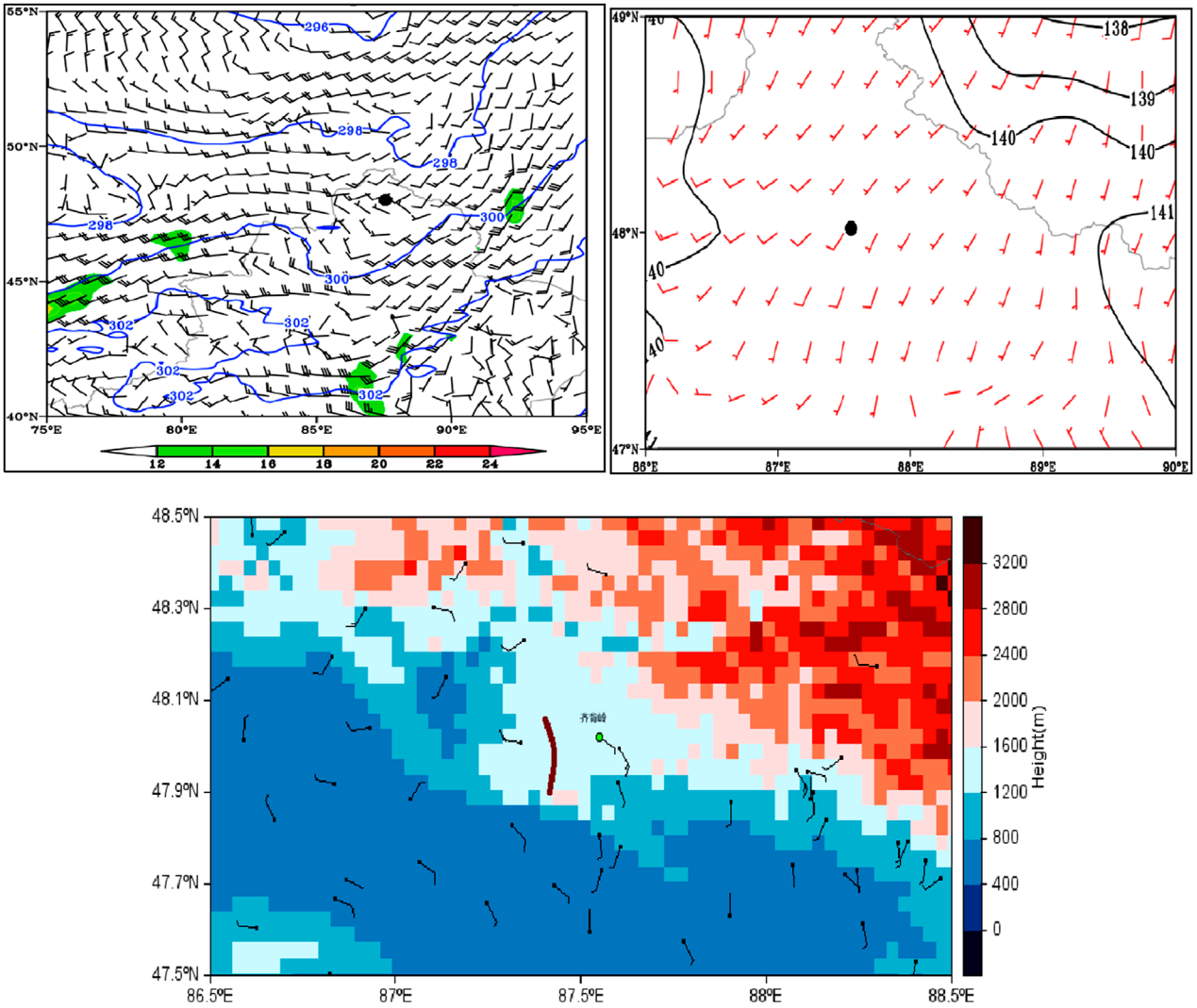

FIGURE 4
Spatial distribution of lower-level geopotential height and wind fields at 11:00 on August 8, 2023: **(a)** 700 hPa, **(b)** 850 hPa (solid lines: geopotential height, unit: dagpm; shaded areas: jet streams, unit: m·s^{-1}; superimposed wind field: m·s^{-1}; ● denotes Qibeiling Station). **(c)** Surface (shaded area: topography, ● denotes Qibeiling Station).

and Kala stations were analyzed using ECWMF model sounding grid data. As shown in Figure 6, at 06:00 GMT on the 8th, two representative stations show a clear warm advection below 500 hPa as the wind direction turns clockwise with height, while above 500 hPa, there is a cold advection with wind direction turns counterclockwise with height. This lower-level warm and upper-level cold stratification created conditions conducive to convective initiation and development. The representative stations have a high Freezing Level (FL) and equilibrium levels (EL), but low Lifting Condensation Level (LCL) indicating low cloud base heights, vertically extensive clouds, and a thick warm cloud layer. These characteristics are favorable for enhancing precipitation efficiency.

According to the stratification parameters, both stations exhibited K-index values exceeding 35°C, with Showalter Index (SI) and Lifted Index (LI), indicating a highly unstable atmosphere; strong Vertical Wind Shear (VWS) shows the presence of intense updrafts within the cloud cluster; the Convective Available Potential Energy (CAPE) at both stations exceeded 1000 J·kg^{-1}, while the Convective Inhibition (CIN) remained below 50 J·kg^{-1}. These metrics showed if sufficient triggering mechanisms were activated, this would lead to the release of unstable energy and the development of severe convective weather. Specific convective parameters for both stations are detailed in Table 1.

4.4 Water vapor transport and convergence

4.4.1 Water vapor transport pathways

By analyzing the whole layer vector integral of water vapor flux from the surface to 300 hPa before and in the middle of the rainstorm, it can be seen that there are two obvious channels for water vapor transport during the rainstorm. The upstream channel is water vapor originated from the Atlantic Ocean, reaching the Black Sea, then followed the western, northern, and eastern flanks of the European blocking high, moved southward to Central Asia,

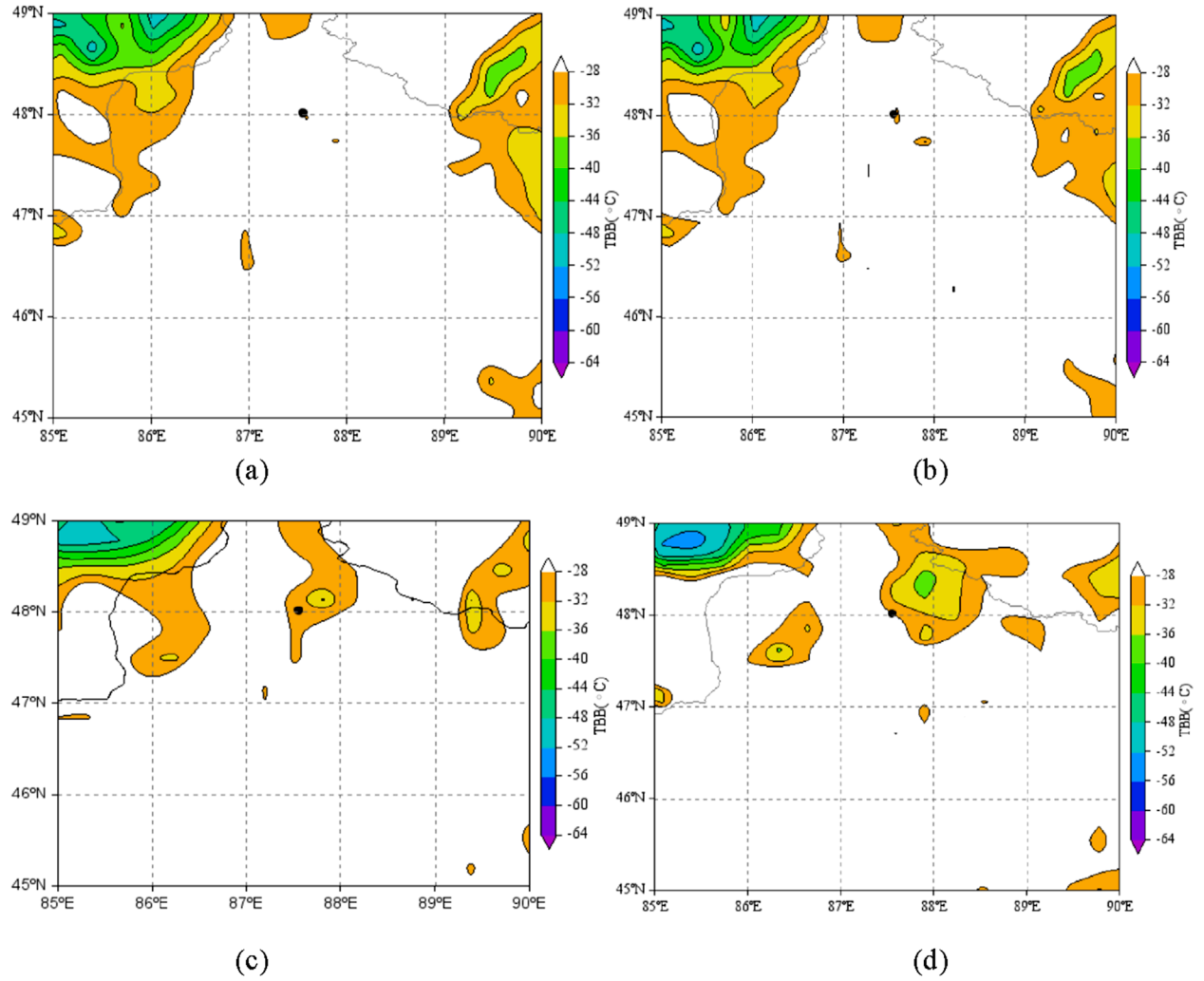

FIGURE 5
Evolution of FY-4A/TBB near Qibeiling Station (black spot) in the center of rainstorm at **(a)** 11:34 **(b)** 11:38 **(c)** 12:00 **(d)** 12:30 GMT (unit: °C) on August 8, 2023.

partially merged with water vapor carried by the Siberian low vortex, and was subsequently relayed to the rainstorm area via pre-trough southwesterly airflow. The downstream channel is influenced by the westward extension and northward thrust of the West Pacific Subtropical High (WPSH), water vapor advanced along the pre-ridge from the Arabian Sea and Bay of Bengal to the eastern Qinghai-Tibetan High, then northwestward through the Hexi Corridor. There, it converged with the pre-trough southwesterly airflow from Central Asia and partially merged with water vapor from the Siberian low vortex.

The primary water vapor source for this rainstorm was both the upstream channel and the inherent water vapor of the influencing systems. Additionally, the persistent maintenance of the Siberian low vortex ensured a continuous supply of water vapor to the rainstorm area (Figures 7a,b).

The entire process of water vapor transport and accumulation is also more distinctly visible. By 12:00 on 6 August, a certain amount of water vapor had already accumulated over the Altay region (Figure 7c). As short-wave troughs split from the Siberian low vortex continuously replenished water vapor, a significant concentration of water vapor was observed over northern Xinjiang by 05:38 on 8 August. High water vapor content persisted in the western and northern parts of the Tacheng-Altay area until 9 August (Figure 7d). The strong spatial correspondence between the primary regions of heavy rainfall and the areas of high-water vapor content indicates that satellite-derived water vapor products are effective in identifying potential zones of heavy rainfall or short-duration intense precipitation.

4.4.2 Vertical distribution and convergence characteristics of water vapor transport

The occurrence of heavy rainfall involves the transport of substantial water vapor to a specific region and its convergence at particular altitudes. To elucidate the spatiotemporal features of water vapor transport pathways and convergence mechanisms in the core area of the rainstorm, a detailed analysis of water vapor flux and convergence intensity was conducted using data from the Qibeiling representative station.

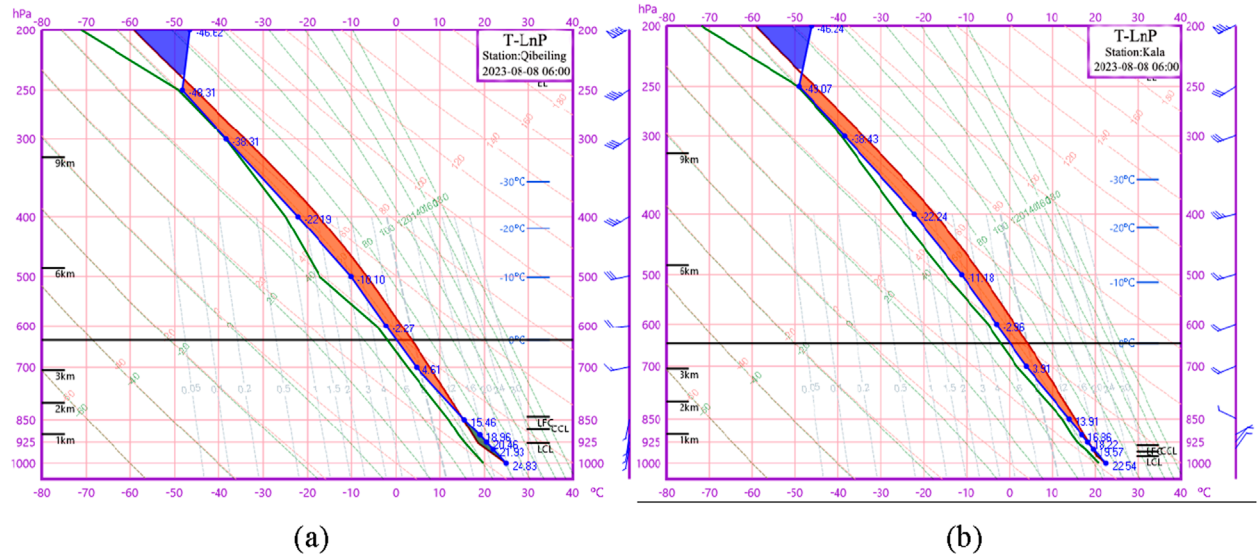

FIGURE 6
ECMWF model soundings at representative stations **(a)** Qibeiling and **(b)** Kala before the heavy rainfall at 06:00 GMT on August 8, 2023.

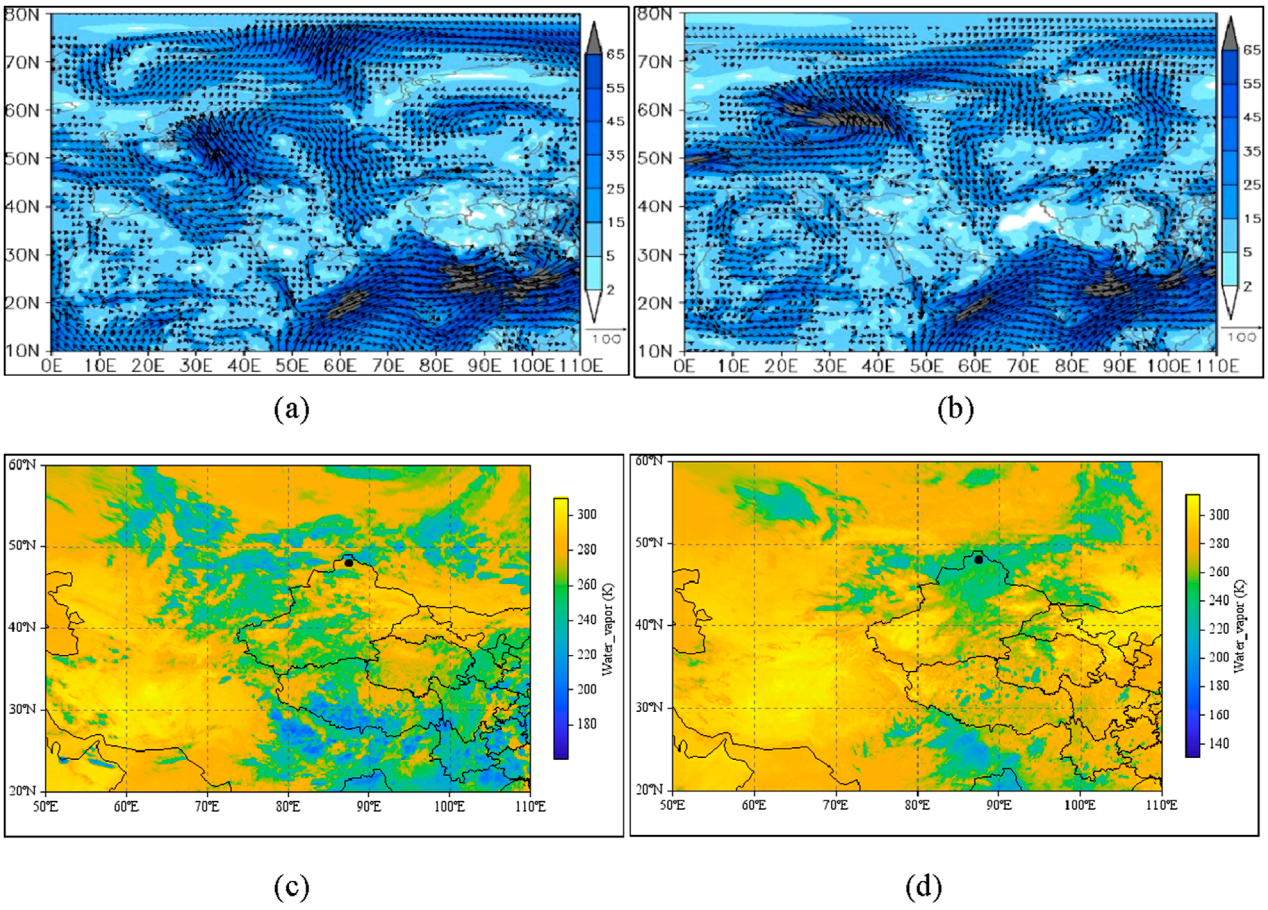

FIGURE 7
The whole layer Water vapor flux integral from the ground to 300 hPa in the rainstorm process (unit: kg·m^{-1}· s^{-1}) at **(a)** 12:00 on the 6th, **(b)** 06:00 on the 8th, and water vapor changes in before and after the rainstorm from FY-4A/TBB Water vapor channel (unit: K) at **(c)** 12:00 on the 6th, **(d)** 06:00 on the 8th in August 2023.

TABLE 1 Key stratification Parameters of Representative Stations at 06:00 on August 8, 2023.

Representative stations	K /°C	SI /°C	LI /°C	VWS /m·s^{-1}·km^{-1}	CAPE /J·kg^{-1}	CIN /J·kg^{-1}	FL /m	EL /hPa	LCL /hPa
Qibeiling	35.5	−0.55	−3.56	0.30	1,273	54	3,920	238	928
Kala	35.2	−1.16	−4.64	0.36	1,504	6	3,778	236	974

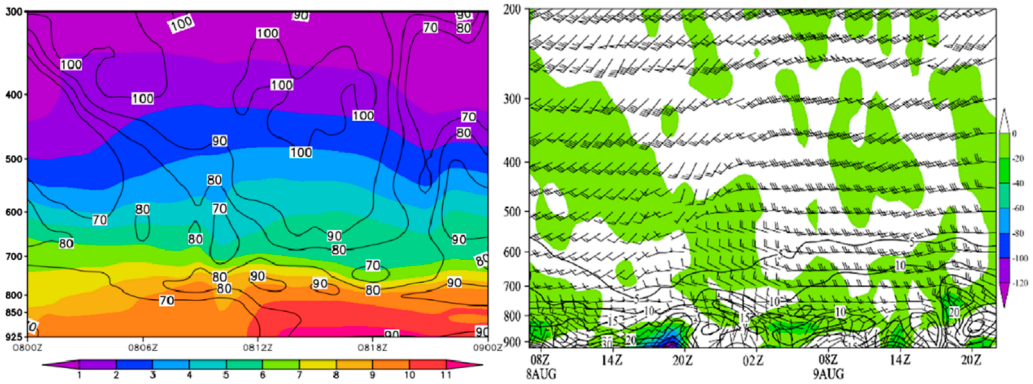

FIGURE 8
Time-height cross-section from ERA5 data at Qibeiling Station from 00:00 on 8 August to 00:00 on 9 August 2023. **(a)** Specific humidity (shaded, units: g·kg^{-1}) overlaid with relative humidity (contours, units: %). **(b)** Water vapor flux (contours, units: 10^{-3} g·cm^{-1}·hPa^{-1}·s^{-1}) and water vapor flux divergence (shaded, units: 10^{-5} g·cm^{-2}·hPa^{-1}·s^{-1}), superimposed with wind vectors (units: m·s^{-1}).

Water vapor transport during the event was predominantly concentrated below 600 hPa. With the highest values observed below 800 hPa, water vapor flux consistently exceeded 1 × 10^{-2} g·cm^{-1}·hPa^{-1}·s^{-1}, peaking around 11:00 on 8 August at 3 × 10^{-2} g·cm^{-1}·hPa^{-1}·s^{-1}. During 06:00–11:00 GMT on 8 August, water vapor convergence intensified below 800 hPa. Near the surface, the water vapor flux divergence reached −1.2 × 10^{-3} g·cm^{-2}·hPa^{-1}·s^{-1}. After 12:00, the divergence rapidly increased, coinciding with a marked reduction in precipitation intensity (Figure 8a).

Analysis of the temporal and vertical variations in water vapor content at the rainstorm core reveals abundant water vapor in the mid-to low-level atmosphere before and during the event. The specific humidity at 700 hPa exceeded 8 g·kg^{-1}, while below 850 hPa, values reached 10 g·kg^{-1} prior to 20:00 on 8 August, significantly higher than those observed during heavy rainfall events in eastern Altay (Zhuang et al., 2017). Relative humidity remained ≥70% throughout the troposphere from 8th to 9th August, sustaining a highly saturated environment until the rainstorm concluded (Figure 8b).

From the above analysis, it can be seen that the water vapor transport and convergence changes exhibited by the center of this rainstorm are compared with the extreme rainstorms occurring in the eastern part of Xinjiang, the northern slope of the Tianshan Mountains, and the northern slope of the Kunlun Mountains, exhibited significantly greater water vapor flux, stronger convergence, shorter duration, a lower altitude of the intense water vapor center, higher water vapor content, and an exceptionally prolonged duration of saturated conditions. These features, historically rare in Xinjiang's rainfall events, provided optimal water vapor conditions for the occurrence of this extreme rainstorm.

4.4.3 Water vapor budget characteristics

To quantify water vapor transport during the rainstorm (7–10 August) over northern Xinjiang's heavy rainfall area (43°–49°N, 70°–90°E), 6-hourly water vapor input and output across different boundaries in total column (from surface to 300 hPa) were calculated. The total column was divided into lower troposphere (surface–700 hPa), middle troposphere (700–500 hPa), upper troposphere (500–300 hPa).

As shown in Figure 9a, the western boundary of the rainstorm area exhibited Total Column Water Vapor (TCWV, hereinafter) influx, characterized by maximum input in the lower troposphere and minimum in the upper troposphere. The pre- and post-rainstorm water vapor input in the lower troposphere displayed wave-like intensification. Water vapor influx fluctuated minimally prior to midday on 8 August, followed by a rapid intensification in lower level from 06:00 to 12:00, which then sharply decreased until 18:00 on the 8th. Subsequently, it gradually intensified again, reaching the peak value of this rainstorm event at 18:00 on the 9th. The middle tropospheric water vapor influx followed a similar trend to the lower layer but with reduced amplitude. In the upper troposphere, insignificant variation trends were observed due to limited water vapor content. The TCWV variations were predominantly influenced by the lower troposphere, exhibiting essentially identical temporal evolution patterns.

The water vapor transport was dominated by outflow, with only a minor influx observed in the lower atmosphere before short-duration heavy rainfall events in northern boundary (Figure 9b). In the eastern boundary, water vapor exhibited persistent outflow throughout the total column (Figure 9c). The middle and upper troposphere maintained predominant water

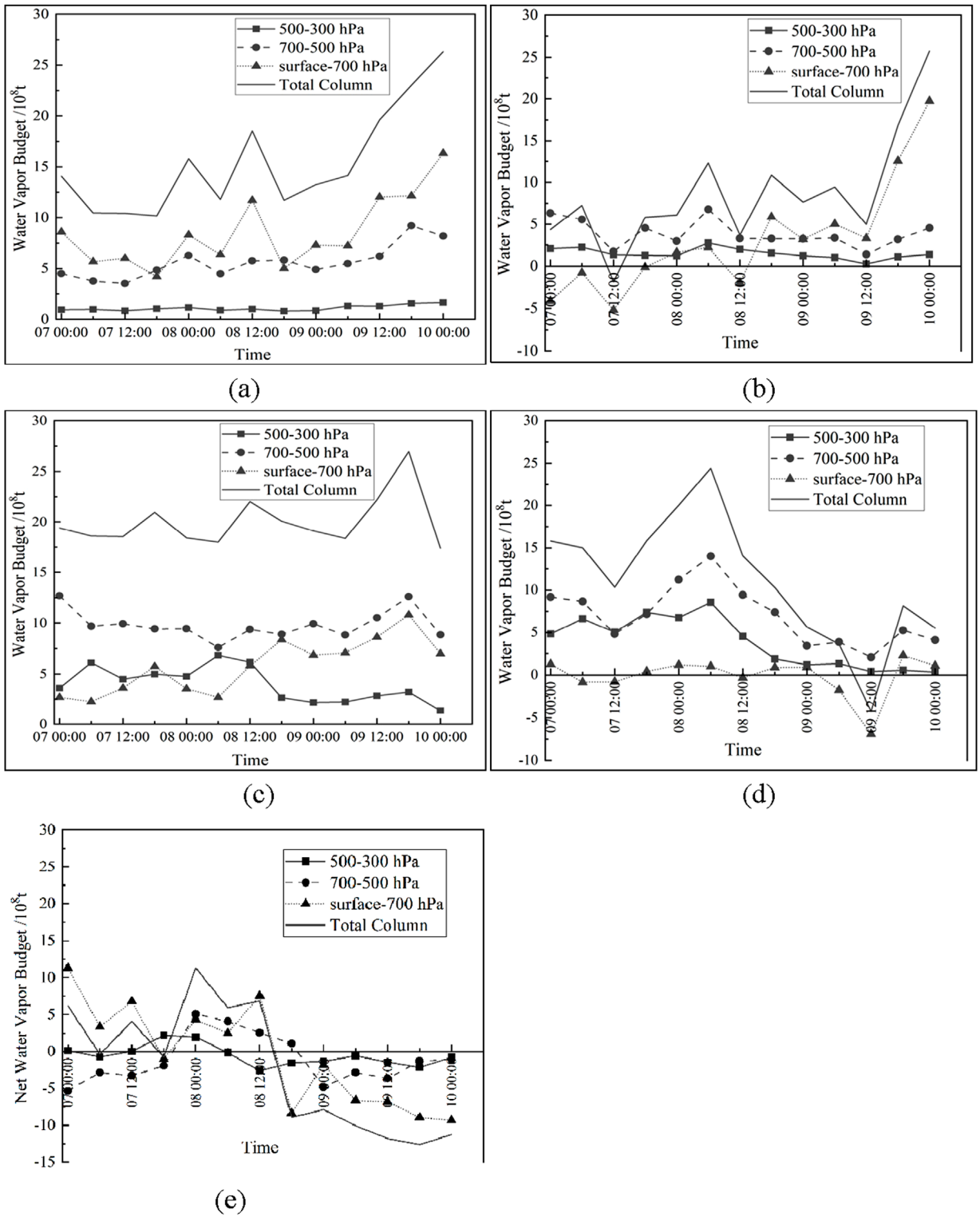

FIGURE 9
Water vapor transport across each boundary at high, middle, low levels and total column of the troposphere from 00:00 on August 7, 2023 to 00:00 on August 10, 2023 on **(a)** Western Boundary **(b)** Northern Boundary **(c)** Eastern Boundary **(d)** Southern Boundary **(e)** region.

vapor influx, characterized by a rapid enhancement from 12:00 on the 7th to 06:00 on the 8th, followed by gradual attenuation. The lower troposphere demonstrated comparatively weaker water vapor influx (Figure 9d). The upper troposphere mainly relied on net water vapor input from 12:00 on the 7th to 06:00 on the 8th, and water vapor output during other times. The change in water vapor in the middle troposphere lags behind that in the upper troposphere about 6 h, and the trend is basically similar. lower troposphere water

vapor input occurred before 12:00 on the 8th, followed by water vapor output (Figure 9e).

From the characteristics of water vapor budget at each boundary, the western boundary is dominated by the predominant water vapor influx, primarily concentrated in the lower troposphere, which is dynamically linked to the eastward progression of weather system. Sustained water vapor influx occurs mainly in the mid-upper troposphere, attributed to the topographic blocking effect of the Tianshan Mountains that impedes southward water vapor transport in the southern boundary. The eastern and northern boundaries are mainly characterized by output. Before the rainstorm, the water vapor in the whole layer is mainly input, which provides abundant water vapor for this heavy rainfall weather.

4.5 Thermodynamic and topographic conditions

From the pseudo-equivalent potential temperature (Θ_{se}) at 850 hPa, it can be seen that on the 8th, the northern part of Altay Region and the Ili and Bortala areas were all located in the high-energy zone with Θ_{se} > 336 K and $\Theta_{se500\text{-}850}$ <-3 K during the daytime. By 08:00, Qibeiling was situated in the high-energy tongue zone, with $\Theta_{se500\text{-}850}$<−8 K. This configuration was maintained for about 2 h, leading to intense precipitation in the region (Sun, 2014) (Figure 10a). On the 9th, the high-energy zones in northern Xinjiang were distributed in a dispersed, patchy manner, corresponding to $\Theta_{se500\text{-}850}$<−4 K all day. The overlap of the high-energy zones or tongues of Θ_{se} with $\Theta_{se500\text{-}850}$ < 0 is one of the main reasons for the instability of the atmospheric stratification, which triggers short-duration heavy precipitation in multiple locations.

Analysis of the Time-Height cross sections of Θ_{se} and temperature advection at the heavy rainfall center reveals that there is a high-energy tongue zone with Θse > 336 K below 800 hPa before and during the heavy rainfall. Meanwhile, around 700–500 hPa, a low Θse zone between 700 and 500 hPa indicated convective instability in the atmosphere. On the temperature advection cross-section, there is strong warm advection spatially correlated with the high-energy tongue below 800 hPa before and during the heavy rainfall, contrasted by pronounced cold advection above 500 hPa. This warm-over-cold vertical configuration provided favorable thermodynamic conditions for convective development, consistent with vertical wind field variations captured in the model sounding at this station (Figure 10b).

From the temporal evolution of horizontal divergence in the vertical direction over the rainfall center, significant convergence zones associated with convective instability area were observed before and during the heavy rainfall. A strong convergence center (-7×10^{-5} s^{-1}) was located near 900 hPa, while divergence dominated above 850 hPa, peaking at 6×10^{-5} s^{-1}. In the vertical velocity field, weak upward motion began in the lower troposphere over the representative station at 04:00 GMT on the 8th. By 10:00–12:00 GMT, this upward motion extended to the mid-upper levels, forming a primary upward velocity center (-1.0 Pa·s^{-1}) near 825 hPa and a secondary center near 450 hPa. Both centers were situated within regions of sharp gradients between strong convergence and divergence. The vertical coupling of these ascending centers, combined with alternating horizontal divergence patterns, enhanced local atmospheric "siphoning effects." Additionally, the tilted structure of vertical velocity and divergence fields favored the development of intense convection (Figure 10c).

The heavy rainfall occurred primarily on the southwestern slopes of the Altai Mountains' foothills, highlighting the critical role of topography. The Altai Mountains slope downward from northwest to southeast. Low-level southerly/southwesterly flows (including a low-level jet) intensified convergence and stagnation near the foothills, promoting water vapor accumulation and uplift. At the surface, cyclonic convergence and strong easterly winds further enhanced convergence as airflow ascended northwestward along the slopes. At Qibeiling Station, located in an area with higher terrain to the northeast and lower terrain to the southwest, local topography amplified vertical ascent and created favorable convergence-divergence patterns. This configuration led to rapid intensification of precipitation. The terrain-driven divergence field near Qibeiling Station exhibited a distinct low-level convergence and upper-level divergence structure, coinciding with maximized upward vertical motion during peak rainfall periods.

Topographically, the heavy rainfall occurred primarily on the southwestern slopes of the Altai Mountains' foothills, highlighting the critical role of topography. The Altai Mountains slope downward from northwest to southeast. Low-level southerly, southwesterly flows (including a low-level jet) intensified convergence and stagnation near the foothills, promoting water vapor accumulation and uplift. At the surface, cyclonic convergence and strong easterly winds further enhanced convergence as airflow ascended northwestward along the slopes. At Qibeiling Station, located in an area with higher terrain to the northeast and lower terrain to the southwest, local topography amplified vertical ascent and created favorable convergence-divergence patterns. This configuration led to rapid intensification of precipitation. The terrain-driven divergence field near Qibeiling Station exhibited a distinct low-level convergence and upper-level divergence structure, coinciding with maximized upward vertical motion during peak rainfall periods.

4.6 Conceptual model of upper- and lower-level configurations for the heavy rainfall

Based on the in-depth analysis of atmospheric circulation, dynamic-thermodynamic conditions, water vapor supply, mesoscale features, and topographic influences, a conceptual model of upper- and lower-level configurations for this heavy rainfall event is illustrated (Figure 11). Specifically, the key components are as follows: above the middle-level atmosphere, establishment of the eastern mode of the South Asian High at 100 hPa; intensification of the upper-level southwesterly jet at 200 hPa; Vigorous development of the upstream European blocking high and downstream East Siberian Ridge, accompanied by the southward and westward displacement of the West Siberian Low Vortex, which continuously split short-wave troughs that merged with the Central Asian trough at 500 hPa. Below the lower level, a southwesterly low-level jet provided abundant water vapor and significant unstable energy to the rainfall area at 700 hPa; high-energy frontal zone and convergence of southwesterly winds with topography enhanced water vapor pooling below 800 hPa.

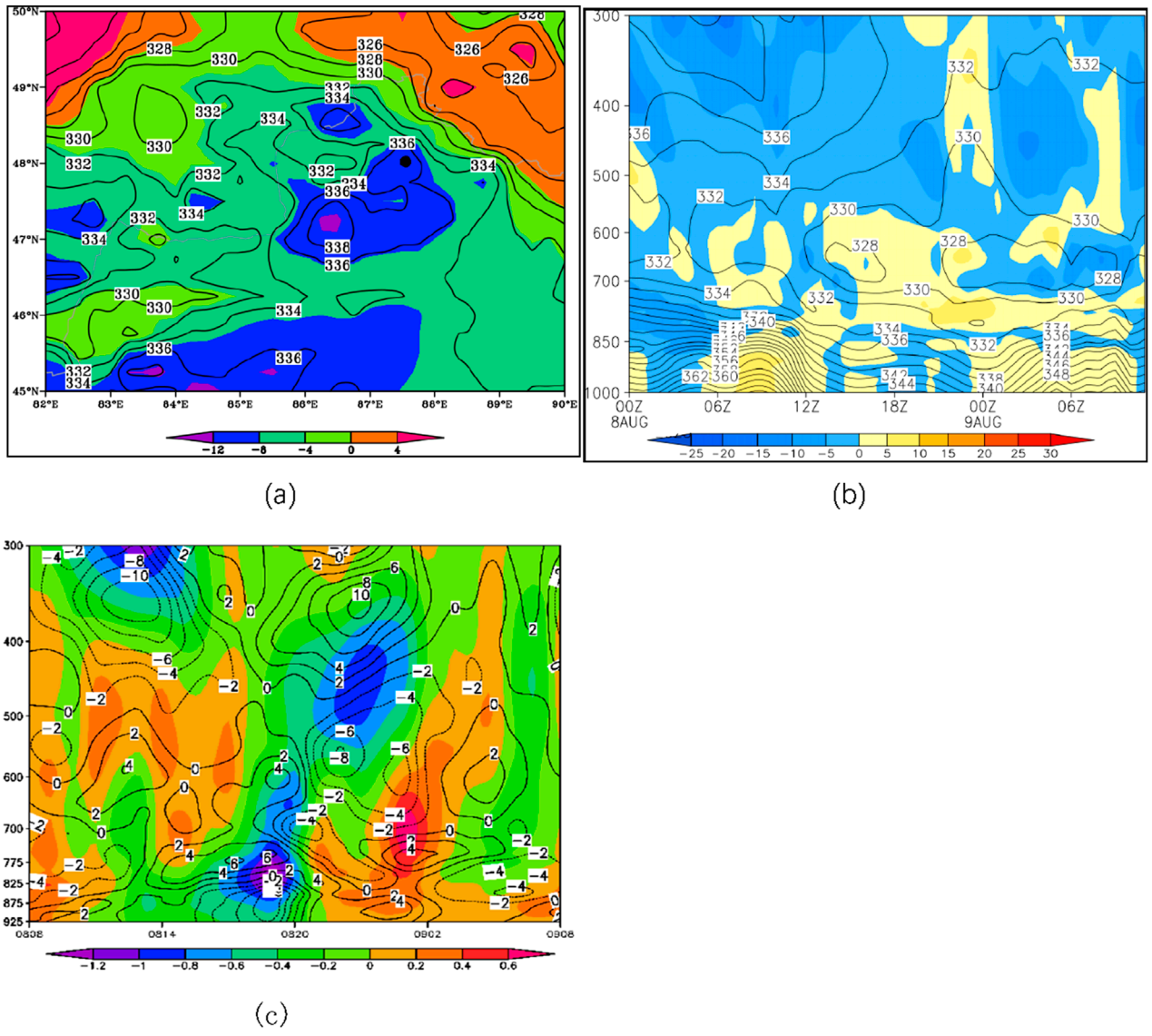

FIGURE 10
(a) Distribution of θ_{se} (contour, unit: K) and $\theta_{se500\text{-}850}$ (shading, unit: K) at 850 hPa at 08:00 GMT on the 8th; **(b)** θ_{se} (contour, unit: K) and temperature advection (shading, unit: 10^{-5} K·s^{-1}) at Qibeiling Station from 00:00 GMT on the 8th to 00:00 GMT on the 9th; **(c)** Tim-Height cross section of horizontal divergence (contour, unit: 10^{-5} s^{-1}) and vertical velocity (shading, unit: Pa·s^{-1}) at Qibeiling Station from 00:00 GMT on the 8th to 00:00 GMT on the 9th.

Vertically, the vertical configuration of alternating convergence (−) and divergence (+) zones from lower to upper levels reached peak intensity simultaneously with upward motion, exhibiting a slightly forward-tilted structure, promoting convective intensification and water vapor uplift.

5 Conclusions and discussion

5.1 Conclusions

This study conducted an in-depth analysis of an extreme heavy rainfall event in northern Xinjiang from 7 to 9 August 2023, utilizing data from automatic weather stations, FY-4A satellite products, NCEP/FNL reanalysis, ERA5, and ECMWF model soundings. The main conclusions are as follows:

(1) The rainfall was caused by the eastern mode of the South Asian High. The West Siberian trough, influenced by the upstream European blocking high and downstream East Siberian Ridge, moved southward and westward, merging with the Central Asian trough. Short-wave troughs ahead of this system moved eastward into northern Xinjiang. A persistent southwesterly low-level jet (LLJ) and its frontal convergence zone, along with shear lines and mesoscale convergence over the rainfall center, supported the development and maintenance of M_{β}CS, creating a favorable environment for extreme rainfall.
(2) The rainfall center had a warm lower-level and cold upper-level stratification. Convective cloud clusters featured low

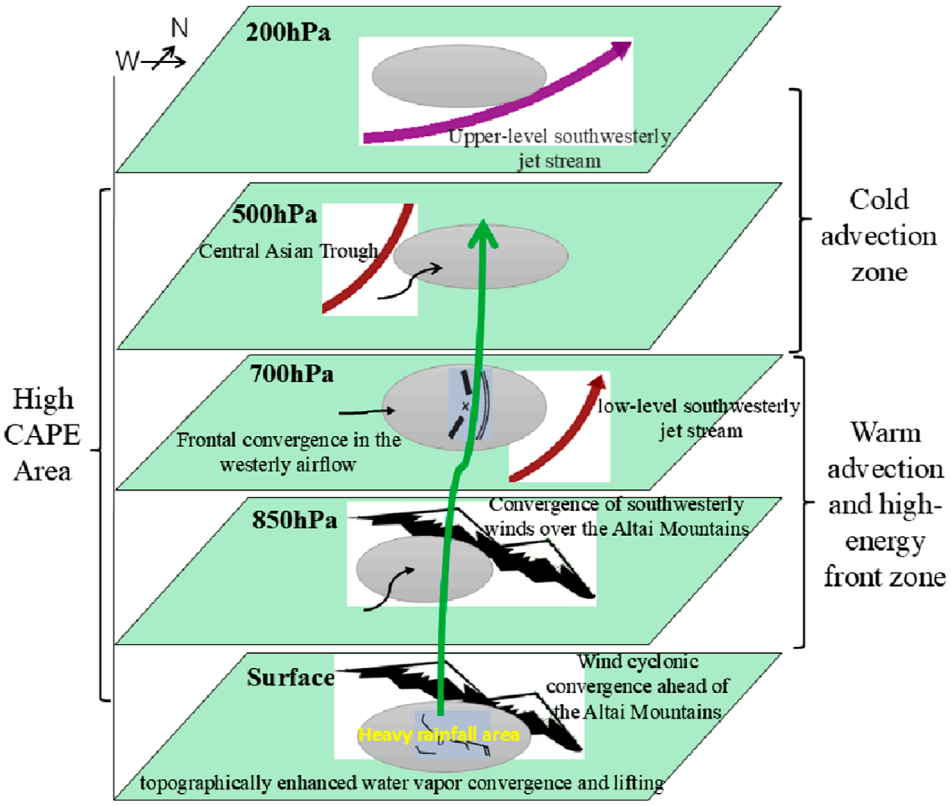

FIGURE 11
Upper-low level configuration model of rainstorm in northern Xinjiang.

cloud bases, high vertical extension, and thick warm cloud layers. Convective indices such as K, SI, LI, CAPE, and CIN indicated significant convective instability, conducive to intense convective weather.

(3) Water vapor supply to the rainfall area came from both upstream and downstream channels, with the upstream channel and synoptic systems dominating. Stable synoptic circulation ensured continuous water vapor transport to the rainfall region. FY-4A/LPW products effectively captured water vapor transport and accumulation processes, matching the spatiotemporal distribution of heavy rainfall. In northern Xinjiang, the western and mid-upper southern boundaries were water vapor inputs, while the eastern and northern boundaries were outputs. The rainfall center had high water vapor flux, strong convergence, short-duration intensification, low-altitude water vapor concentration, and prolonged saturation, providing optimal water vapor conditions for extreme precipitation.

(4) The coexistence of a low-level high-energy zone and transient maintenance of $\theta_{se500\text{-}850} < 0$ triggered short-duration heavy rainfall at multiple locations. Mesoscale convergence and shear in low-level and surface wind fields released unstable energy. The Altai Mountains and local topography near Qibeiling Station synergistically enhanced water vapor transport, convergence-divergence patterns (low-level convergence and upper-level divergence), vertical ascent, and cyclonic surface convergence. These factors peaked simultaneously, amplifying rainfall intensity.

5.2 Discussion

The occurrence of this heavy rainfall event in northern Xinjiang resulted from the synergistic effects of multi-scale systems under an anomalous Central Asian circulation background. From the perspective of atmospheric circulation configuration, heavy rainfall in Xinjiang is often associated with a bimodal SAH at 100 hPa (Zhang et al., 1986). However, during this event, the South Asian High exhibited an eastern mode, which facilitated the establishment, maintenance, and southward extension of the pre-trough southwesterly jet. The rainfall primarily occurred in Altay and Ili in northern Xinjiang, consistent with findings from previous studies (Zhang et al., 2015). Notably, the intensity of the European blocking high during this event remained between 588 and 584 dagpm, comparable to historical extreme rainfall events on the northern slopes of the Tianshan Mountains (Chen et al., 2012).

The persistent eastward movement of short-wave troughs split from the Central Asian trough—driven by coordinated upstream and downstream high-pressure systems—served as the primary synoptic background. However, the widespread heavy rainfall across multiple stations suggests that the atmospheric environment in the study area was characterized by widespread instability and abundant water vapor, both of which were validated through detailed analysis of atmospheric stratification and water vapor conditions.

Comparative analysis of atmospheric stratification over the rainfall center using EC model soundings, ERA5 reanalysis,

and FY-4A/TBB products revealed vertical wind shear and thermal advection confirmed a warm lower-level and cold upper-level structure. Cloud-top brightness temperatures (TBB ≤ −40°C) and equilibrium heights indicated deep convective cloud clusters with high vertical extension. High CAPE values and sustained near-surface updrafts suggested subsequent energy release, leading to localized high-energy tongues and intense short-duration rainfall. Statistical analysis of convective parameters at representative stations prior to the rainfall event confirmed thresholds for short-duration heavy precipitation (Zhuang et al., 2018).

While water vapor for Xinjiang rainfall typically originates from westerly flows and local evaporation, this event exhibited a dual-channel convergence of upstream and downstream water vapor sources. Combined with the unique topography of the Altai Mountains, abundant water vapor converged and ascended along the southern foothills, resulting in water vapor flux and convergence intensities exceeding those of other foothill rainfall events. Although water vapor transport was dominated by upstream systems, the prolonged contribution from the downstream channel played a critical role in sustaining precipitation.

By comparing with previous research on extreme precipitation processes in the region, it was found that this precipitation process has the novel characteristics as follows. Firstly, this process has a wide impact range and high precipitation intensity. Unlike the previous weather pattern of a southward high-pressure system, this process is mainly of the eastern type of the southward high-pressure system. The convergence of mountain front airflow triggers the mesoscale convective system, resulting in local rainstorm weather. Most areas in northern Xinjiang have an unstable atmospheric layer with abundant water vapor present.

Since there was no weather radar in Altay where the rainstorm center was located at that time, this paper uses FY-4A products to discuss the changes of mesoscale cloud clusters and water vapor transport and convergence, which demonstrated strong alignment with ground observations, highlighting their potential for monitoring extreme weather in radar-blind zones. However, the 15-min temporal resolution of FY-4A full-disk observation mode limits the detection of finer mesoscale features and rapid water vapor variations. Additionally, Xinjiang's location at the edge of the satellite's coverage hindered effective monitoring of water vapor transport west of 50°E.

Conclusions drawn from this single case study are inherently limited. Recent advancements in Xinjiang's meteorological infrastructure—including over 3,000 automatic weather stations, more than 30 radars, and vertical profiling systems—provide a robust foundation for future real-time monitoring and research. Next, we will use multi-source observation data fusion and numerical simulation to deepen the understanding of extreme precipitation mechanisms in arid areas and improve the predictability of heavy rainfall system over complex terrain.

The shortwave trough is the main influencing system of extreme summer precipitation weather in northern Xinjiang. When analyzing, forecasters often focus on the location and intensity of low troughs (vortex) but tend to overlook the heavy precipitation weather caused by the rapid eastward movement of shortwave troughs. In addition, the distribution of such rainstorm centers is related to the local terrain height, and it is not uncommon to see cases of short-term heavy precipitation caused by the local uplift and convergence of warm and humid air flow. Therefore, emergency disaster reduction departments need to timely grasp the direction of local flash floods and prevent the harm caused by heavy rainfall floods to downstream areas.

Data availability statement

The original contributions presented in the study are included in the article/supplementary material, further inquiries can be directed to the corresponding author.

Author contributions

JL: Funding acquisition, Writing – original draft, Formal Analysis. BL: Data curation, Formal Analysis, Writing – original draft. CJ: Investigation, Methodology, Supervision, Writing – original draft. YJ: Data curation, Writing – review and editing, Visualization. JZ: Writing – review and editing, Data curation, Visualization. LY: Writing – review and editing, Funding acquisition, Investigation, Supervision. NL: Writing – review and editing, Funding acquisition, Data curation, Visualization.

Funding

The author(s) declare that financial support was received for the research and/or publication of this article. This research was funded by the Key Research and Development Task Special Project of Xinjiang Uygur Autonomous Region (2022B03027-1), Science and Technology Development Fund of Institute of Desert Meteorology, Urumqi, China Meteorological Administration (KJFZ202504), Key Scientific Research Project of Xinjiang Meteorological Bureau (ZD202505), and the Tianshan Mountains Talent Project (2022TSYCLJ0003).

Acknowledgments

The authors are thankful for the assistance and good suggestions of Zhuang Xiaocui, Chen Jin, and other colleagues who took part in this work.

Conflict of interest

The authors declare that the research was conducted in the absence of any commercial or financial relationships that could be construed as a potential conflict of interest.

Generative AI statement

The author(s) declare that no Generative AI was used in the creation of this manuscript.

Publisher's note

References

Bradley, A. A., and Smith, J. A. (1994). The hydrometeorological environment of extreme rainstorms in the southern plains of the United States. *J. Appl. Meteorology* 33 (12), 1418–1431. doi:10.1175/1520-0450(1994)033<1418:theoer>2.0.co;2

Bull, L. J., Kirkby, M. J., Shannon, J., and Hooke, J. (2000). The impact of rainstorms on floods in ephemeral channels in southeast Spain. *Catena* 38 (3), 191–209. doi:10.1016/s0341-8162(99)00071-5

Chen, C. Y., Kong, Q., and Li, R. Q. (2012). Analysis of a major rainstorm in the north slope of Tianshan mountains. *Meteorol. Mon.* 38 (1), 72–80. doi:10.7519/j.issn.1000-0526.2012.01.008

Chen, D., Lei, G., and Jiang, X. W. (2010). Characteristics of large-scale circulation background of summer heavy rainfall in Sichuan during 1981—2000. *Trans. Atmos. Sci.* 33 (4), 443–450.

Chessa, P. A., Ficca, G., Marrocu, M., and Buizza, R. (2003). Application of a limited-area short-range ensemble forecast system to a case of heavy rainfall in the mediterranean region. *Weather and Forecast.* 19 (3), 566–581. doi:10.1175/1520-0434(2004)019<0566:aoalse>2.0.co;2

Deng, W., Chen, H. B., Ma, Z. S., Tian, H. W., Zhang, Y. T., Shen, Z. Y., et al. (2009). Decoding and graphic display of the ncep fnl global analysis data. *Meteorological Environ. Sci.* 32 (3), 78–82. doi:10.1007/BF01390126

Dolaite, X. (2005). The classification of precipitation levels in Xinjiang. *Desert Oasis Meteorology* 28 (3), 7–8. doi:10.3969/j.issn.1002-0799.2005.03.003

Dragani, R., Hersbach, H., Poli, P., Pebeuy, C., Hirahara, S., Simmons, A., et al. (2015). Recent reanalysis activities at ECMWF: results from ERA-20c and plans for ERA5. *Abstract retrieved from Agu Fall Meeting Abstracts, San Francisco, CA (A11R.02)*.

Gregersen, I. B., Madsen, H., Rosbjerg, D., and Arnbjerg-Nielsen, K. (2014). Long term variations of extreme rainfall in Denmark and southern Sweden. *Clim. Dyn.* 44 (11-12), 3155–3169. doi:10.1007/s00382-014-2276-4

Hirockawa, Y., and Kato, T. (2012). Kinetic energy budget analysis on the development of a meso-β-scale vortex causing heavy rainfall, observed over aomori prefecture in northern Japan on 11 november 2007. *J. Meteorological Soc. Jpn.* 90 (6), 905–921. doi:10.2151/jmsj.2012-604

Houze, R. A., Smull, B. F., and Dodge, P. (1990). Mesoscale organization of springtime rainstorms in Oklahoma. *Mon. Wea. Rev.* 118 (118), 613–654. doi:10.1175/1520-0493(1990)118<0613:moosri>2.0.co;2

Hyun, B. K., Song, K. C., Jung, S. J., Sonn, Y. K., Kim, L. Y., et al. (2007). Assessment of environmental impact on the severely soil-eroded area by heavy rainfall. *Korean J. Soil Sci. Fertilizer* 40 (2), 118–130. doi:10.13140/2.1.3174.8482

Japay, D. R., Che, G., and Li, R. Q. (2007). Analysis of summer heavy rainfall in eastern xinjiang. *Meteorol. Mon.* 33 (02), 64–71. doi:10.7519/j.issn.1000-0526.2007.02.010

Jiang, C. L., Guo, Q., Li, J. G., and Li, Y. (2013). A preliminaryanalysis of formational causes of a heavy rain in north slope of tianshan mountain. *J. Arid Land Resour. Environ.* 27 (6), 160–166.

Jiang, Y. F., Qin, J. X., Baheti, M., and Chen, X. (2024). Diagnosis and analysis of the causes of the 3.13 heavy rainfall in yili, xinjiang. *Clim. Change Res. Lett.* 13 (1), 129–138. doi:10.12677/ccrl.2024.131014

Keim, B. D. (2010). Record precipitation totals from the coastal new england rainstorm of 20–21 october 1996. *Bull. Am. Meteorological Soc.* 79 (6), 1061–1067. doi:10.1175/1520-0477(1998)079<1061:rptftc>2.0.co;2

Kong, Q., Zheng, Y. G., and Chen, C. Y. (2011). Synoptic scale and mesoscale characteristics of 7·17 urumqi heavy rainfall in 2007. *J. Appl. Meteorological Sci.* 22 (1), 12–22.

Lapo, P., Barodka, S., and Krasouski, A. (2017). Heavy rain forecasts in mesoscale convective system in july 2016 in Belarus. *EGU General Assem. Conf.*

Li, H. H., Min, Y., Li, A. B., and Li, R. Q. (2022). Comparative analysis of on water vapor characteristics of two extreme rainstorms in the north slope of kunlun mountains. *Arid. Land Geogr.* 45 (3), 715–724. doi:10.12118/j.issn.1000-6060.2021.397

Lima, J. L. M. P., and Singh, V. P. (2002). The influence of the pattern of moving rainstorms on overland flow. *Adv. Water Resour.* 25 (7), 817–828. doi:10.1016/s0309-1708(02)00067-2

Morin, E., Harats, N., Jacoby, Y., Arbel, S., Getker, M., Arazi, A., et al. (2007). Studying the extremes: hydrometeorological investigation of a flood-causing rainstorm over Israel. *Adv. Geosci.* 12, 107–114. doi:10.5194/adgeo-12-107-2007

Shin, U., and Lee, T. Y. (2015). Origin, evolution and structure of meso-α-scale lows associated with cloud clusters and heavy rainfall over the Korean peninsula. *Asia-Pacific J. Atmos. Sci.* 51 (3), 259–274. doi:10.1007/s13143-015-0076-3

Song, G., Li, X., Jiang, J., Xun, X. Y., Chen, L., and Ma, S. Y. (2015). Procession and causes of the extreme rainstorm event in inner Mongolia in july 2012. *Plateau Meteorol.* 34 (1), 163–172. doi:10.7522/j.issn.1000-0534.2013.00148

Stankov, B. B. (1998). Multisensor retrieval of atmospheric properties. *Bull. Am. Meteorological Soc.* 79 (9), 1835–1854. doi:10.1175/1520-0477(1998)079<1835:mroap>2.0.co;2

Sun, J., Lei, L., Yu, B., and Ding, Q. L. (2015). The fundamental features of extreme heavy rain events in recent 10 years in Beijing area. *J. Meteorological Res.* 73 (4), 609–623.

Sun, J. S. (2014). *Basic principles and technical methods of severe convective weather forecasting*. Beijing: China Meteorological Press.

Trivedi, D., Sharma, O., and Pattnaik, S. (2024). Minimization of forecast error using deep learning for real-time heavy rainfall events over Assam. *Ieee Geoscience Remote Sens. Lett.* 21, 1–4. doi:10.1109/lgrs.2024.3378517

Wang, M. Y., Ding, C. C., Ren, F. M., Zhang, D., and Jia, L. (2023). Heavy rainfall forecast of landfalling tropical cyclone over China with an upgraded DSAEF_LTP model. *J. Geophys. Res. Atmos.* 128 (21). doi:10.1029/2022jd038192

Yadav, B., Kumar, N., and Rathore, L. S. (2021). Skill of operational forecast of heavy rainfall events during southwest monsoon season over India. *Mausam* 66 (3), 579–584. doi:10.54302/mausam.v66i3.564

Yang, L. M. (2003). Research on a case of heavy rain in xinjiang from south asia high abnormity. *Meteorol. Mon.* 29 (8), 21–25. doi:10.1007/BF02948883

Yu, H. Z., and Meng, Z. Y. (2016). Key synoptic-scale features influencing the high-impact heavy rainfall in beijing, China, on 21 july 2012. *Tellus a Dyn. Meteorology Oceanogr.* 68 (1), 31045. doi:10.3402/tellusa.v68.31045

Zeng, Y., Zhou, Y., and Yang, L. (2019). A preliminary analysis of the formation mechanism for a heavy rainstorm in western xinjiang by numerical simulation. *J. Atmos. Sci.* 43 (2), 372–388. doi:10.3878/j.issn.1006-9895.1804.18106

Zhang, J. B., and Deng, Z. F. (1987). *Introduction to precipitation in xinjiang*. Beijing: China Meteorological Press.

Zhang, J. B., Su, Q. Y., and Sun, S. Q. (1986). *Guidelines for short-term weather forecast in Xinjiang*. Urumqi, Xinjiang: Xinjiang People's Publishing House.

Zhang, Y., Li, H., Lin, X., Abulimiti, and Yu, B. (2015). Analysis of continuous rainstorm circulation background and the dynamic process of synoptic-scale in west of southern Xinjiang. *Meteorol. Mon.* 41 (7), 816–824. doi:10.7519/j.issn.1000-0526.2015.07.003

Zhang, Y. H., and Wang, Y. (2004). Analysis of heavy rainfallin southern Hami,Xinjiang. *Meteorol. Mon.* 30 (7), 41–43. doi:10.7519/j.issn.1000-0526.2004.7.009

Zhao, L., Tang, Y. B., and Gao, K. (2017). An analysis on global circulation anomalies and forming mechanism in the preceding month of persistent heavy rainfall events over the south of Yangtze river valley. *J. Trop. Meteorology* 33 (4), 548–557. doi:10.16032/j.issn.1004-4965.2017.04.012

Zhuang, X., Li, R., Li, B., Li, J., and Sun, Z. (2017). Analysis on rainstorm caused by Central Asian vortex in northern Xinjiang. *Meteorol. Mon.* 43 (8), 924–935.

Zhuang, X. C., Xu, Z. Q., and Li, B. Y. (2024). DB 65/T 4831—2024 Short-term heavy rainfall level in xinjiang

Zhuang, X. C., Zhao, J. W., Li, B. Y., and Xie, X. Q. (2018). Characteristics of short-time heavy precipitation weather flow and environmental parameter of altay region in xinjiang. *Plateau Meteorol.* 37 (3), 675–685. doi:10.7522/j.issn.1000-0534.2017.00061

Ziv, B. (2001). A subtropical rainstorm associated with a tropical plume over africa and the middle-east. *Theor. Appl. Climatol.* 69 (1-2), 91–102. doi:10.1007/s007040170037